Supplement to empirical model of global climate: 1. reduced impact of volcanoes upon consideration of ocean circulation

T. Canty [1], N. Mascioli [1], M. Smarte [1], and R. J. Salawitch [1]

[1]{University of Maryland, College Park, MD}

Correspondence to: T. Canty (tcanty@atmos.umd.edu)

1 Supplement

Section 2.2 states "As shown in the Supplementary Material, use of SOD from NOAA rather than SOD from GISS in our regression has no bearing on our finding regarding the sensitivity of $\Delta T_{VOLCANO}$ to the AMO." This point is illustrated in Fig. S1, identical to Fig. 10 of the main paper except the stratospheric optical depth (SOD) record from NOAA (Amman et al., 2003) is used. The NOAA record of SOD is available only to the end 2008. We have extended this record to the end of 2011 by using the last available measure of SOD, 1.8×10^{-4}, for all months after December 2008, so that the regressions in Fig. S1 cover the same time period as the regressions in Fig. 10. Comparison of the arrows on Fig. S1, which denote maximum SOD after the four major eruptions since 1900 (Santa María, Mount Agung, El Chichón, and Mount Pinatubo marked as SM, A, C, and P), to those on Fig. 10 reveals considerable difference between peak SOD in the NOAA record compared to the GISS record (Sato et al., 1993) after major eruptions. This difference is apparent also in Fig 2.18 of IPCC (2007), as noted in Section 2.2 of the main paper. However, maximum cooling due to Pinatubo (the product of C_1 and SOD) is quite similar for both SOD records, because the regression is most sensitive to the timing of the SOD perturbation, which is nearly identitcal for the two data sets. The sensitivities of $\Delta T_{VOLCANO}$ to whether AMO is used in the regression as well as the method used to detrend the AMO are both readily apparent in Fig. S1.

Section 3.2.2 states "in the Supplementary Material, we show simulations for different time series of NAA RF_i, all having NAA $RF_{2005} = -1.0$ W m^{-2}, based on values of α_{COOL} and α_{HEAT} at the intersection of the red line and the "High Road", "Middle Road", and "Low

Road" of Fig. 4." Figure S2 illustrates this point. Regressions in Fig. S2 are all related to Fig. 6d, a regression of the CRU4 global temperature anomaly found using $AMO_{Had3\ AF}$. In the main paper, we used values of the scaling parameters, α_{COOL} and α_{HEAT}, for NAA $RF_{2005} = -1.0$ W m^{-2} along the "Middle Road" of Fig. 4. All regressions shown in Fig. S2 use NAA $RF_{2005} = -1.0$ W m^{-2} as well as $AMO_{Had3\ AF}$. Panel ***a*** of Fig. S2 uses values of α_{COOL} and α_{HEAT} along the "Low Road" of Fig. 4; panel ***b*** is for values of these parameters along the "Middle Road", and panel ***c*** is for values along the "High Road". The tremendous similarity of these regressions supports our contention that the important factor for our analysis is the value of NAA RF_{2005}, rather than the specific combination of α_{COOL} and α_{HEAT} used to arrive at this value. We have conducted extensive testing of these scaling parameters and the central importance of NAA RF_{2005} is robust. As described in the main paper, year 2005 was chosen as the benchmark because of the IPCC (2007) focus on estimating NAA RF for this year. Our entire analysis hardly differs if we had used 2011 as the benchmark. Indeed, as stressed in Mascioli et al. (2012), better definition of the uncertainty in net anthropogenic aerosol radiative forcing, for the contemporary atmosphere, is vital for reducing uncertainties inherent in global warming projections.

Section 3.2.3 states "in Supplementary Material, we show that our overall conclusions are unaffected if KaplanSST2 is used rather than HadSST3". This point is illustrated by Fig. S3, identical to Fig. 10 except the SST record from KaplanSST2 has been used for the definition of AMO. A detailed comparison of Fig. S3 with Fig. 10 reveals only extremely slight differences.

Section 4.3 states "as shown in the Supplementary Material, the derivative of OHC from Church et al. (2011), an update to the record of Domingues et al. (2008), bears no relation to SOD (hence, the conclusion of Murphy et al. (2009) seems highly dependent on which OHC record is used, and possibly how the data are smoothed)" as well as "also, there is no suggestion that when SOD achieves a local maximum (i.e., peak volcanic perturbation), the AMO is at a local minimum either coincident in time with peak SOD (as suggested by GCM of Booth et al., 2012), ~2 to 3 years after peak SOD (as suggested by GCM of Stenchikov et al., 2009), or ~10 years after peak SOD (as suggested by GCM of Zanchettin et al., 2012) (see Supplementary Material)." Figure S4 shows the GISS time series of SOD (panel ***a***), the time derivative of Ocean Heat Content (OHC) data from Church et al. (2011) which equals OHE (e.g., Murphy et al., 2009) (panel **b**), and a scatter plot of these two physical quantities (panel

c). For the scatter plot, we relate SOD to the value of OHE six months into the future, to represent the adjustment time of the stratosphere to the RF perturbation induced by the volcano. Enhanced values of SOD associated with the eruptions of Agung, El Chichón, and Pinatubo as well as OHE (6 month delay) are color coded using the same palette as Fig. 8. This is no significant relation between SOD and OHE. The conclusion of no relation between SOD and OHE holds for 0 time shift, a time shift of 1 year, or any other time shift. Certainly there are valleys in OHE that could plausibly be related to SOD, such as the dip around 1968 that could be related to Agung. Zanchettin et al. (2012) describe the possibility of a 10 year delay between volcanic perturbation and ocean response. However, the OHE record shown in Fig. S4 exhibits 6 well defined, decadal time scale valleys, between 1950 and 2010. In contrast, the SOD record exhibits only 3 strong peaks during this same period of time.

Murphy et al. (2009) describe a visual relation between OHE and SOD, where OHE was found after applying an "8 year linear fit smoothing" to the OHC data of Domingues et al. (2008). We have computed OHE using running means of 3, 5, 7, and 9 years applied to the OHC data of Church et al. (2011) and we still find no significant relation between OHE and SOD. Murphy et al. (2009) do not justify use of "8 year linear fit smoothing" to the OHC record.

Measurements of OHC vary over time, either due to noise in the estimate or perhaps the stochastic nature of atmosphere to ocean heat transfer when examined on a yearly basis. Regardless, the data records we have examined show no evidence for volcanic influence on ocean circulation, despite the indication for such an influence from several independent GCM studies (Stenchikov et al., 2009; Booth et al., 2012; Zanchettin et al., 2012).

Section 4.3 also states "as shown in Supplementary Material, this plot looks similar for $AMO_{Had3\ SST}$ and $AMD_{Had3\ Lin}$, except the AMO is much closer to neutral after the eruption of Santa María when detrended using SST". Figures S5 and S6 are identical to Fig. 8 expect $AMO_{Had3\ SST}$ (Fig. S5) and $AMO_{Had3\ Lin}$ (Fig. S6) are used rather than $AMO_{Had3\ AF}$. The subscripts SST, LIN, and AF refer to various ways of detrending the AMO, as described in Section 3.2.3. All of the AMO records are based on North Atlantic SSTs (HadSST3) from the Hadley Center (Kennedy et al., 2011a,b), denoted by use of Had3 in the subscript. Together Fig. S5, Fig. S6, and Fig. 8 can be used to make two important points: 1) when SOD was enhanced following the four major eruptions since 1900, as well as 6 months before each eruption, the AMO tended to be more negative than positive regardless of how the AMO is

detrended; 2) the value of the AMO index in the early 20th century is most sensitive to how the detrending is conducted. Smaller values of $\Delta T_{VOLCANO}$ are found using $AMO_{Had3\ Lin}$ or $AMO_{Had3\ AF}$, compared to AMOHad3 SST, due to the sensitivity of the regression coefficients to the value of the AMO after the eruption of Santa Maria in October 1902. As discussed in the main paper, observed cooling during the pre-WWI time period and warming during the WWII time period is modeled better using $AMO_{Had3\ Lin}$ or $AMO_{Had3\ AF}$ than $AMO_{Had3\ SST}$, supporting the possibility these representations of the AMO are valid for the early 20th century.

Section 5.1 of the paper states "Nearly all of this perturbation occurs in the tropics: the net radiative effect of Pinatubo poleward of 20° latitude was small in the northern hemisphere and essentially zero in the southern hemisphere (see Supplementary Material)." Figure S7 shows the perturbation to SW, LW, and Net (LW−SW) radiation at the top of the atmosphere measured by ERBE. There is no discernable change in the Net budget, following the eruption of Pinatubo, poleward of 20°S. The SW and LW components each show an effect, but the changes in these components are balanced. As noted in the main paper, the treatment of the stratospheric response of this anomaly (the LW perturbation is due to absorption of thermal radiation within the stratosphere by volcanic aerosols, and re-radiation in all directions) and the downward influence is critical. The perturbations to SW and LW are more distinct in the Northern Hemisphere extra-tropics, but the Net perturbation is hard to distinguish from the noise in the climate system (i.e., without the gray shading or knowledge of when Pinatubo erupted, volcanic influence on the Net budget would be hard to discern).

References

Booth, B. B. B., Dunstone, N. J., Halloran, P. R., Andrews, T., and Bellouin, N.: Aersosols implicated as a prime driver of twentieth-century North Atlantic climate variability, Nature, 484, 228−232, doi:10.1038/nature10946, 2012.

Church, J. A., White, N. J., Konikow, L. F., Domingues, C. M., Cogley, J. G., Rignot, E., Gregory, J. M., van den Broecke, M. R., Monaghan, A. J., and Velicogna, I.: Revisiting the Earth's sea-level and energy budgets from 1961 to 2008, Geophys. Res. Lett., 38, L18601, doi:10.1029/2011GL048794, 2011.

Domingues, C. M., Church, J. A., White, N. J., Glecker, P. J., Wijffels, S. E., Barker, P. M., and Dunn, J. R.: Improved estimates of upper-ocean warming and multidecadal sea-level rise, Nature, 453, 1090–1093, doi:10.1038/nature07080, 2008.

IPCC, 2007: Climate Change 2007: The Physical Science Basis. Contribution of Working Group I to the Fourth Assessment Report of the Intergovernmental Panel on Climate Change [Solomon, S., Qin, D., Manning, M., Chen, Z., Marquis, M., Averyt, K. B., Tignor, M., and Miller, H. L. (eds.)], Cambridge University Press, Cambridge, United Kingdom and New York, NY, USA, 996 pp., 2007.

Kennedy J. J., Rayner, N. A., Smith, R. O., Saunby, M. and Parker, D. E.: Reassessing biases and other uncertainties in sea-surface temperature observations since 1850 part 1: measurement and sampling errors, J. Geophys. Res., 116, D14103, doi:10.1029/2010JD015218, 2011a.

Kennedy J. J., Rayner, N. A., Smith, R .O., Saunby, M. and Parker, D. E.: Reassessing biases and other uncertainties in sea-surface temperature observations since 1850 part 2: biases and homogenization, J. Geophys. Res., 116, D14104, doi:10.1029/2010JD015220, 2011b.

Mascioli, N. R., Canty, T., and Salawitch, R. J., An empirical model of global climate: 2. Implications for future temperature, Atmos. Chem. Phys. Discuss., submitted, 2012.

Murphy, D. M., Solomon, S., Portmann, R. W., Rosenlof, K. H., Forster, P. M., and Wong, T.: An observationally based energy balance for the Earth since 1950, J. Geophys. Res., 114, D17107, doi:10.1029/2009JD012105, 2009.

Sato, M., Hansen, J. E., McCormick, M. P., and Pollack, J. B.: Stratospheric aerosol optical depths, 1850–1990. J. Geophys. Res., 98, 22987–22994, doi:10.1029/93JD02553, 1993.

Stenchikov, G., Delworth, T. L., Ramaswamy, V., Stouffer, R. J., Wittenberg, A., and Zeng, F.: Volcanic signals in oceans, J. Geophys. Res., 114, D16104, doi:10.1029/2008JD011673, 2009.

Zanchettin, D., Timmreck, C., Graf, H.-F., Rubino, A., Lorenz, S., Lohmann, K., Kruger, L., Jungclaus, J. H.: Bi-decadal variability excited in the coupled ocean-atmosphere system by strong tropical volcanic eruptions, Clim. Dyn., 39, 419−444, doi:10.1007/s00382-011-1167-1, 2012.

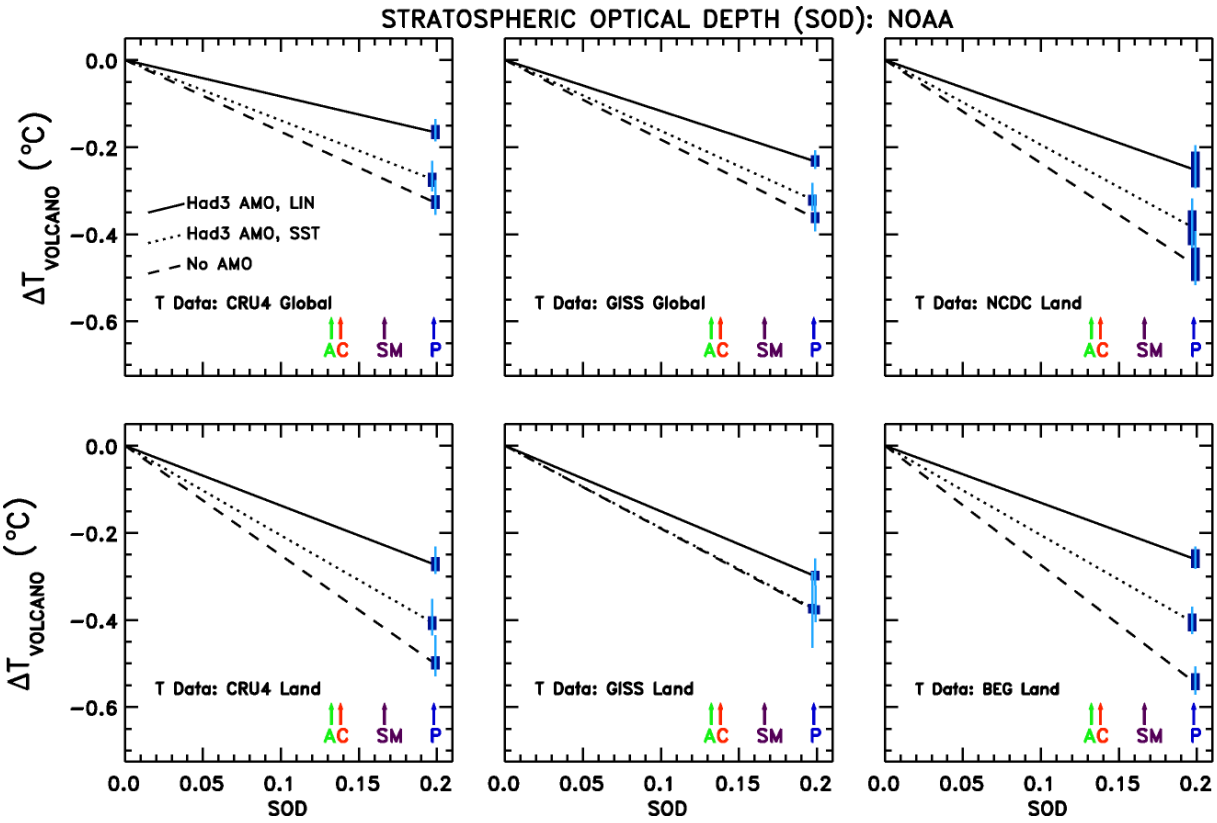

Fig. S1. Same as Fig. 10 in the main paper, except the NOAA record of SOD from Amman et al. (2003) is used.

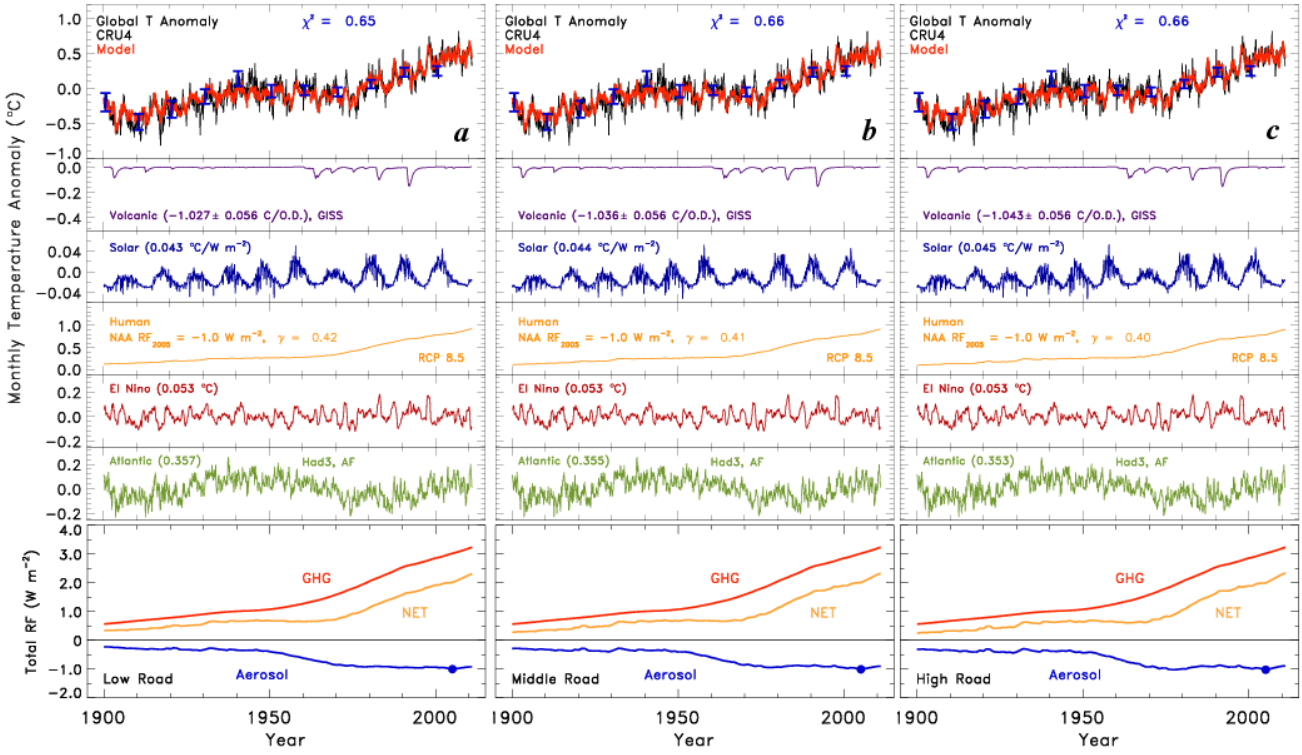

Fig. S2. Same as Fig. 6d in the main paper except we have excluded here rungs of the ladder plots showing PDO and IOD (these terms are small) and we have added a panel (lowest rung) showing time series of NAA RF, GHG RF, and the net anthropogenic RF. **(a)** Regression using NAA $RF_{2005} = -1.0$ W m^{-2} for values of α_{COOL} and α_{HEAT} along the "Low Road" of Fig. 4. **(b)** Regression using NAA $RF_{2005} = -1.0$ W m^{-2} for values of α_{COOL} and α_{HEAT} along the "Middle Road" of Fig. 4 (this regression is identical to that shown in Fig. 6d of the main paper). **(c)** Regression using NAA $RF_{2005} = -1.0$ W m^{-2} for values of α_{COOL} and α_{HEAT} along the "High Road" of Fig. 4. All regressions use $AMO_{Had3\ AF}$ (see main text).

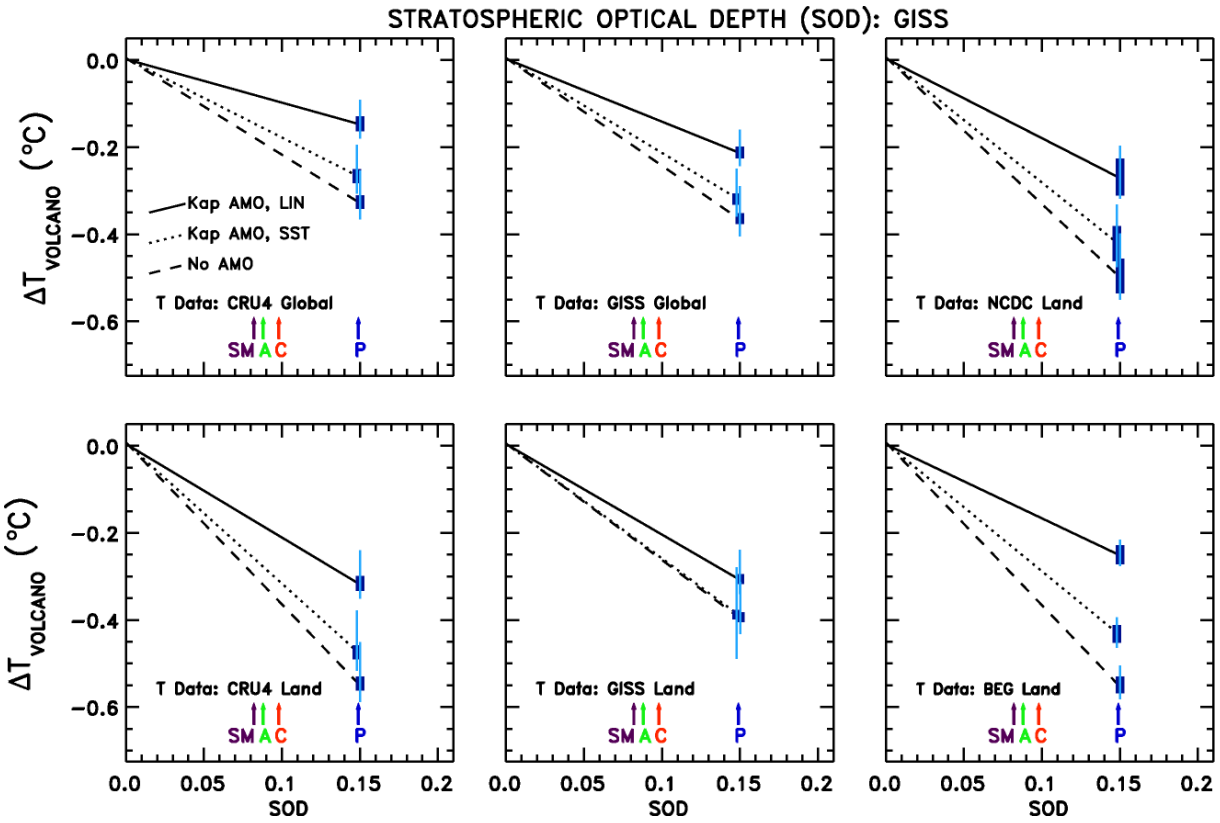

Fig. S3. Same as Fig. 10 in the main paper, except the Kaplan Extended SST V2 record from NOAA (Kaplan et al., 1998; Enfield et al., 2001; see also Appendix B) has replaced HadSST3 for the definition of the AMO.

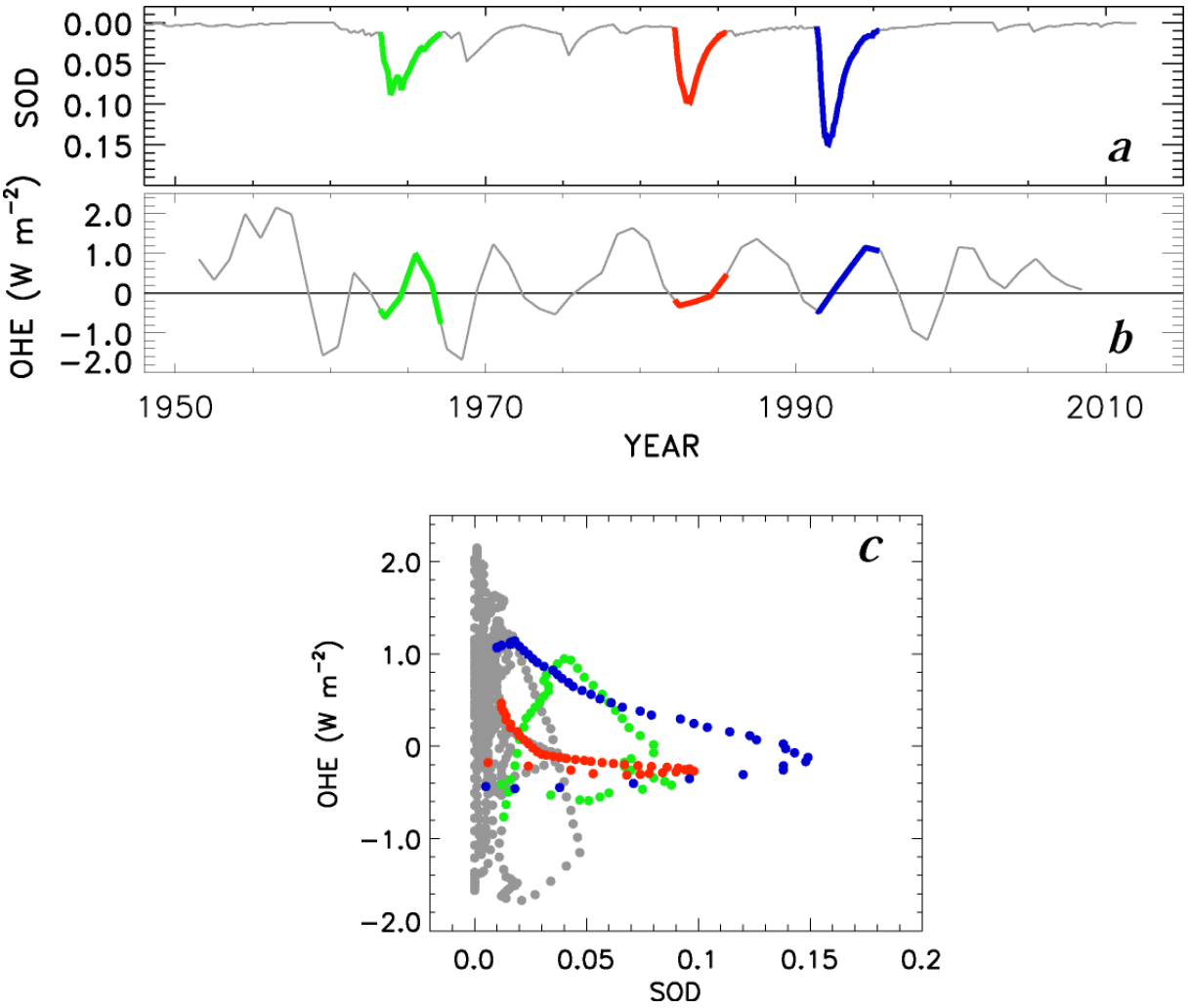

Fig. S4. (a) Monthly mean stratospheric optical depth (SOD) from Sato et al. (1993). The three major volcanoes since 1950, Mount Agung (green), El Chichón (red), and Mount Pinatubo (blue) are indicated. **(b)** Ocean Heat Export (OHE) found by taking the derivative with respect to time of the Ocean Heat Content (OHC) record of Church et al. (2011). OHC is provided in an annual basis.

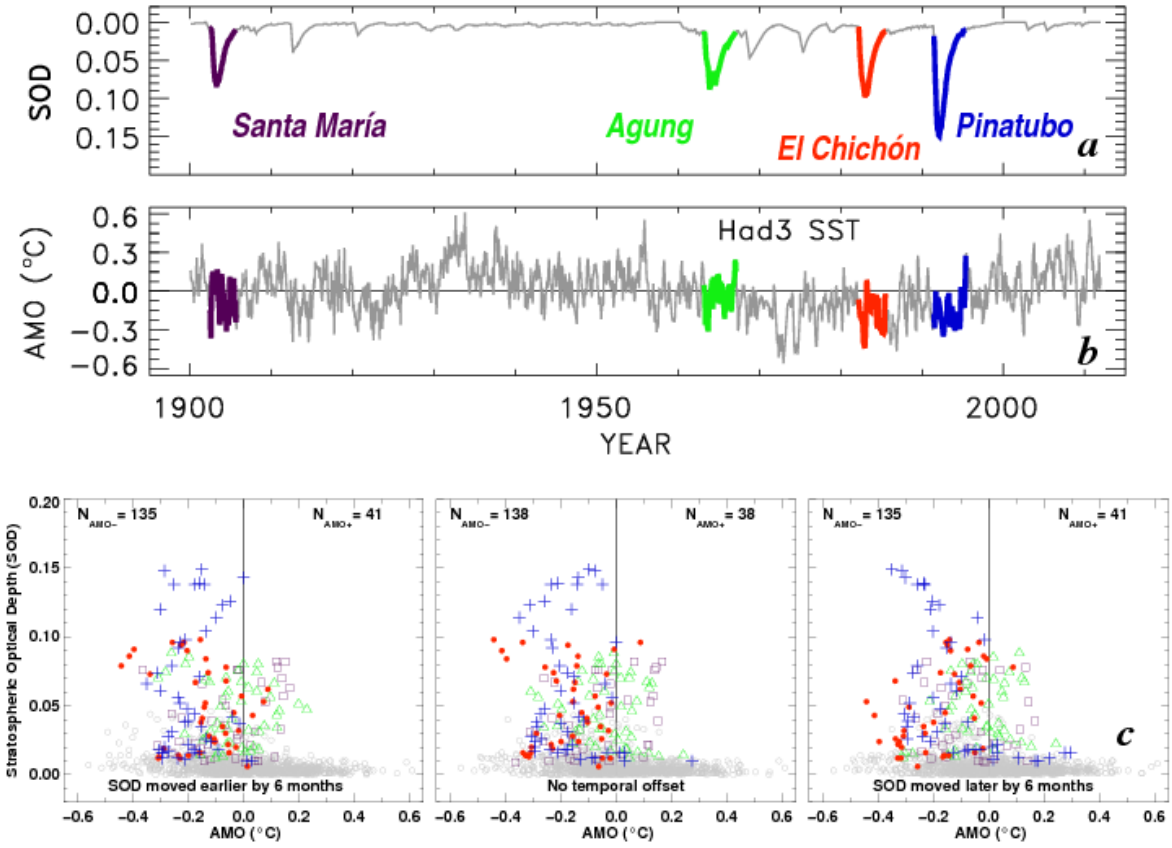

Fig. S5. Same as Fig. 8 except $AMO_{Had3\ SST}$ is used, rather than $AMO_{Had3\ AF}$.

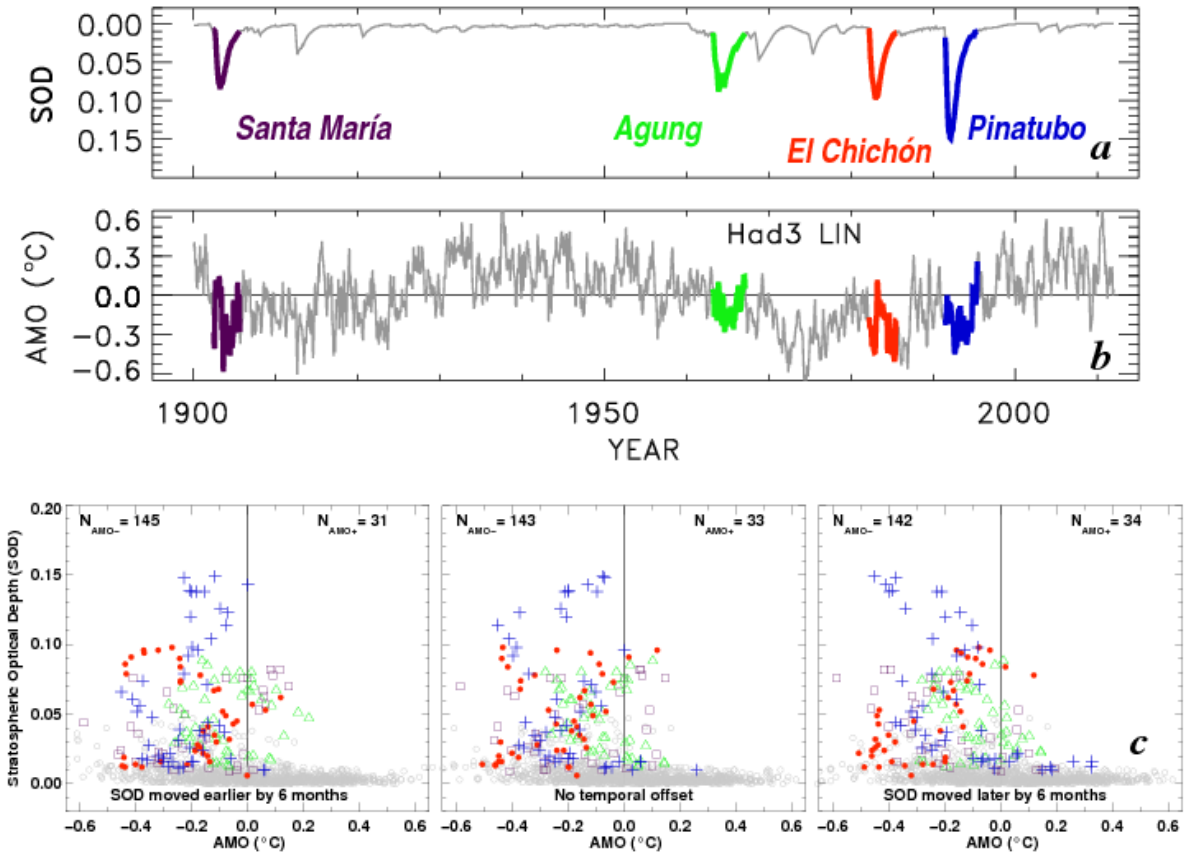

Fig. S6. Same as Fig. 8 except $AMO_{Had3\ LIN}$ is used, rather than $AMO_{Had3\ AF}$.

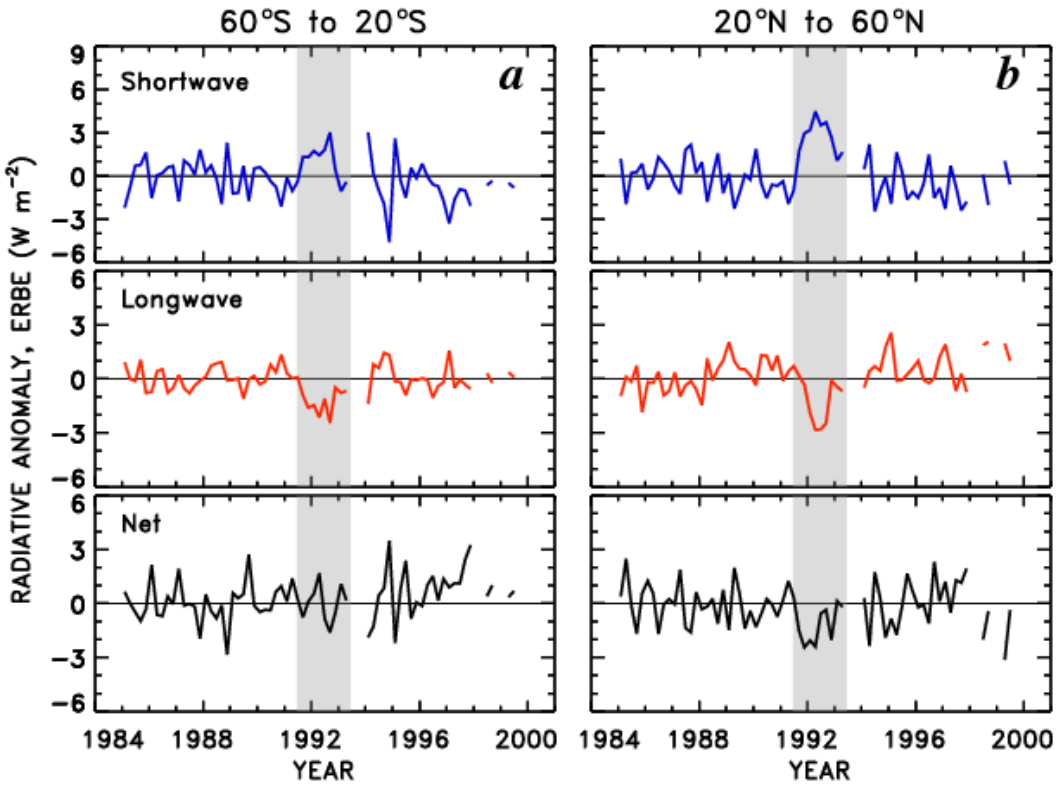

Fig. S7. Same as Fig. 13 except for the 60°S to 20°S and the 20°N to 60°N latitude regions. Analysis based on raw data provided as 72-day means.